Quantifying SARS-CoV-2 Omicron variant spread and the impact of non-pharmaceutical interventions in Newfoundland and Labrador, Canada

Francis Anokye[1*], Michael WZ Li[2,3], Steve Walker[3‡], Amy Hurford[4,5]

1 Interdisciplinary - School of Graduate Studies, Memorial University of Newfoundland, St. John's, NL, Canada
2 Science Policy Integration Branch, Public Health Agency of Canada, Guelph, Ontario, Canada
3 Department of Mathematics and Statistics, McMaster University, Hamilton, Ontario, Canada
4 Department of Mathematics and Statistics, Memorial University of Newfoundland, St. John's, NL, Canada
5 Department of Biology, Memorial University of Newfoundland, St. John's, NL, Canada

*Correspondence Email: fanokye@mun.ca

Author Contributions

Francis Anokye: Conceptualization, Methodology, Software, Formal analysis, Visualization, Writing – original draft, Writing – review & editing.
Michael W.Z. Li: Conceptualization, Methodology, Software, Writing – review & editing.
Steve Walker: Software, Methodology, Review & editing.
Amy Hurford: Conceptualization, Methodology, Funding acquisition, Supervision, Writing – review & editing.

Abstract

The highly transmissible Omicron variant of SARS-CoV-2 caused many infections in Newfoundland and Labrador (NL), and the fraction of infections that were unreported varied as PCR testing capacity was exceeded and eligibility rules changed. Due to these inconsistencies in the testing rate, we developed a mechanistic model that was calibrated to seroprevalence data (Dec 2021–May 2022) to estimate underreporting and understand the impact of non-pharmaceutical interventions on transmission. Our model considers the epidemiology of SARS-CoV-2 spread, natural and vaccine-derived immunity, and the booster dose vaccination campaign that was ongoing in NL during the study. We found that during the early spread of the Omicron variant, when the eligibility for tests that were reported in the provincial counts was less restrictive, fewer than 3 infections were unreported per reported case. After March 17, 2022, when test eligibility was more restrictive, the underreporting rate increased steadily, with an average of 21 infections unreported infections per reported case. We found that Omicron transmission was lower when schools were closed (mean reproduction number, $\mathcal{R}_0 = 1.44$, 95% CI: 1.41–1.47), higher when open (mean $\mathcal{R}_0 = 2.03$, 95% CI: 1.60–2.46), and of the alert levels, ALS-4 reduced transmission the most (mean $\mathcal{R}_0 = 1.52$, 95% CI: 1.35–1.69). When underreporting rates vary, the impact of non-pharmaceutical

interventions, such as alert level systems and school closures, cannot be determined from reported cases. Our findings highlight the value of combining seroprevalence data with modelling to determine the impact of NPIs during pandemics when surveillance systems are constrained. ALS-4 reduced spread the most

Author summary

Reported COVID-19 cases often underestimate the number of infections, especially when testing capacity is exceeded or eligibility rules change. This occurred in Newfoundland and Labrador (NL), Canada, during the spread of the Omicron variant, when testing rates were uneven and many infections were unreported. Our analysis showed that underreporting increased substantially when eligibility for tests that could be reported in the official counts was restricted to high-risk individuals and people who work with high-risk individuals. Given this eligibility change, the underreporting ratio increased from 3 to an average of 21 unreported infections per reported case. We used an epidemiological model to account for the many factors, such as asymptomatic infections and vaccination status, that are known to affect infection spread. We found that transmission was lower when schools were closed, higher when schools were open, and of the alert levels, ALS-4 reduced spread the most. These results highlight that reported cases alone can produce inaccurate results when testing systems are constrained and the rate of testing is variable. Using our approach of combining serological data with modelling enabled us to evaluate the impact of public health measures. These results support knowledge mobilization to explain to the public why particular public health measures are being implemented during an emergency.

Introduction

COVID-19, caused by the SARS-CoV-2 virus, initiated a public health emergency, and as the virus spread, new variants emerged, some of which were variants of concern due to their increased transmissibility and virulence, and the diminished impact of public health measures and vaccines against their spread (1). In November 2021, the Omicron (B.1.1.529) variant (2) emerged and, due to its high transmission and immune evasion, challenged the effectiveness of surveillance programs (3) and non-pharmaceutical interventions (NPIs) (4; 5; 6) even in regions such as the province Newfoundland and Labrador (NL), Canada, that had effectively controlled previous variants and vaccinated a high percentage of their populations (7; 8).

Throughout the pandemic, Canadian provinces and territories required that individuals meeting specific requirements, usually at least one COVID-19 symptom, schedule a Polymerase Chain Reaction (PCR) test to identify SARS-CoV-2 infection. The results of these PCR tests were the basis of reported cases in Canada. During the spread of the Omicron variant, PCR test capacity became limited and the provinces and territories adapted by changing the requirements for testing and relying on rapid antigen tests (9), the results of which were usually not reported in official counts (10). These changes increased the proportion of SARS-CoV-2 infections that were not included in the official counts.

Reported cases can produce inaccurate epidemiological curves when the proportion of cases that are unreported changes over time. Serosurveillance can address this challenge by estimating infection prevalence more consistently than PCR testing. PCR tests return positive results when viral load is sufficiently high to be detected by the assay (11), while serosurveillance can occur by testing blood samples to identify the antibodies to SARS-CoV-2. Seroconversion refers to an antibody concentration that is

high enough to be detected and seroreversion refers to antibody concentrations that can no longer be detected due to waning (occurs over a period of approximately 3–4 months (12)). During the COVID-19 pandemic, serosurveillance was often completed as a cross-sectional survey of blood donors (13). As compared to PCR testing, serosurveillance is less likely to miss asymptomatic infections. Limitations of serosurveillance are whether the blood donor populations are representative of the population, particularly as blood donation has its own eligibility criteria (e.g., age, health status, travel history, and behavioural risk factors), that blood donation centers can be inaccessible to residents of remote and rural populations, and that surveys conducted after antibodies have waned will not detect infections.

Serosurveillance identifies both asymptomatic and symptomatic infections and can be compared to reported cases to estimate under-reporting rates. From March to May 2020, a longitudinal serosurvey of ten sites in the United States identified 6-24 more infections as compared to official counts (14), and serosurveys in British Columbia, Canada, found a substantial increase in underreporting after March 2022 (15).

An epidemic curve where the chance of infections being reported is constant over time is necessary for retrospective studies of control measures to limit infection spread. Such measures are pharmaceutical interventions, i.e. vaccination, and NPIs such as programs of test-trace-isolate, social distancing, capacity limits, mask mandates and recommendations, travel measures and suspending some activities, where school closures are often given particular consideration. Studies show that stricter or earlier implementation of NPIs lowered transmission and hospitalizations even in highly vaccinated populations (5; 16). School closures were often linked with decreases in transmission and hospitalizations due to COVID-19, though the strength of the effect varied by country and timing (5; 16).

In this study, we developed a mechanistic compartmental model stratified by vaccination status, which we calibrated to infection-induced seroprevalence data from December 2021 to May 2022. This approach allowed us to quantify how underreporting varied over time as PCR testing capacity was exceeded and eligibility rules became more restrictive. We estimated the time-varying transmission rate and calculated the reproduction number to evaluate the impact of NPIs. Our analysis quantifies the impact of NPIs on the spread of the Omicron variant, in a small, highly vaccinated population that had experienced few SARS-CoV-2 infections from prior variants.

Methods

Data

Our analysis covers the period from December 15, 2021 to May 22, 2022 and considers: (i) infection-induced seroprevalence estimates, and (ii) daily reported case counts. Seroprevalence estimates were used for model calibration to estimate infections, which was used to determine the impact of NPIs and combined with reported cases to estimate underreporting ratios. We interpreted all infections reported during this period as the BA.1 Omicron variant (see Sec. S1.1 in S1 Text for justification).

Seroprevalence estimates

From April 2020 to March 2024, the Covid-19 Immunity Task Force (CITF) centralized Canadian SARS-CoV-2 immunity data (17). CITF conducted periodic serological surveys across Canada using three primary sources: (1) blood donors from Canadian Blood Services and Héma-Québec, (2) anonymized discarded or residual blood samples from provincial laboratories, and (3) participants in CITF-funded research cohorts (13).

Reported case counts

COVID-19 daily reported cases are publicly available on the Public Health Agency of Canada's website (18), but for this study were provided by the data custodian, the Newfoundland and Labrador Centre for Health Information (NLCHI, now part of NL Health Services – Digital Health), under Health Research Ethics Board approval (2021.013). We applied a left-aligned 7-day moving average to the reported cases. On January 9, 2022, the NL government reported 1009 cases, which were tests that had occurred weeks earlier and had been sent out of the province for analysis. This reporting anomaly affects estimates of the underreporting ratio prior to this date.

NPIs implemented in NL during the spread of Omicron

NL implemented NPIs of varying strictness, which were described by the COVID-19 Alert Level System (ALS) (19; 20) that had been developed at the beginning of the public health emergency (Sec. S1.2 in S1 Text for a complete summary of the ALS system in NL). Of the alert levels that were implemented during our study period, Alert level 2 (ALS-2) was the least strict alert level, alert level 3 (ALS-3) was of intermediate strictness, and alert level 4 (ALS-4) was the strictest, consisting of the lowest capacity limits and more suspended activities. After March 14, 2022, all ALS measures were lifted (No-ALS), as the end of the public health emergency declaration occurred at this time. K–12 schools closures were separate from the ALS system. K–12 schools were closed at times during the study period, partly due to the regular winter break (December 23, 2021 to January 3, 2022), and partly due to recommendations from the Department of Health and Community Services that closed schools for an additional 3 weeks (see Sec. S1.3 in S1 Text for details).

Shortly after the establishment of the Omicron variant in NL, PCR testing was exceeded. As capacity continued to be strained, eligibility rules for PCR tests that were reported in the official counts continued to change. Initially, in December 2021, testing was mandatory for anyone with symptoms or identified as a contact (T1), but by March 17, 2022, eligibility was restricted to only symptomatic individuals that were also high-risk or that could spread infection to high-risk individuals (adults over 60, individuals in congregate settings, pregnant women, immunocompromised individuals, and healthcare workers; T5 see Sec. S1.4 of S1 Text). The periods of ALS levels, K–12 school operational status and changes to PCR testing rules are shown in Fig 1.

Model

To understand the impact of NPIs implemented in NL after the establishment of the Omicron variant, we estimated the time-varying transmission rate using a mechanistic Susceptible-Exposed-Asymptomatic-Infected-Recovered (SEAIR) compartmental model (Fig 2 and equations S1 Text in Sec. S1.5). Our model is similar to the structures in earlier studies (21; 22; 23) and is stratified into three population cohorts according to vaccination status (we do not distinguish between vaccine types e.g., mRNA vs. viral vector or brand-specific products), where each cohort has its own SEAIR compartments. The vaccination cohorts are individuals who are: unvaccinated or partially vaccinated (i.e., one dose from a two dose primary series; denoted with a subscript 1); fully vaccinated (i.e., have received the primary series of a Health Canada-approved COVID-19 vaccine, denoted with a subscript 2); booster-vaccinated (i.e., have received additional shots (one or more) to complement the primary series, denoted with a subscript 3).

We assumed that all cohorts mix equally and have the same contact rates. Asymptomatic infections are scaled by a constant, ζ, to reduce the chance of infection

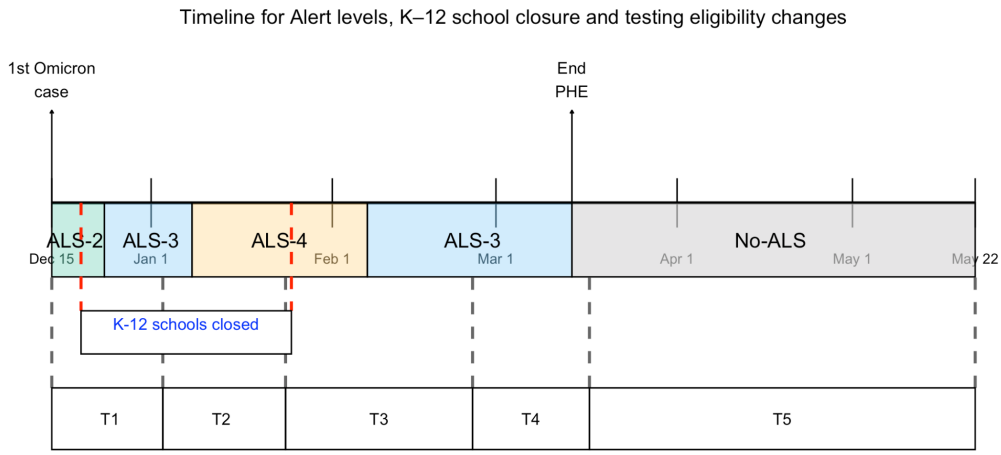

Fig 1. Timeline of alert levels, K–12 school closure, and testing eligibility changes (Dec 15, 2021–May 22, 2022). 'End PHE' is the end of the Public Health Emergency declaration. T1–T5 are periods of different PCR test eligibilities. See Sec. 1.2-1.4 in S1 Text) for additional details.

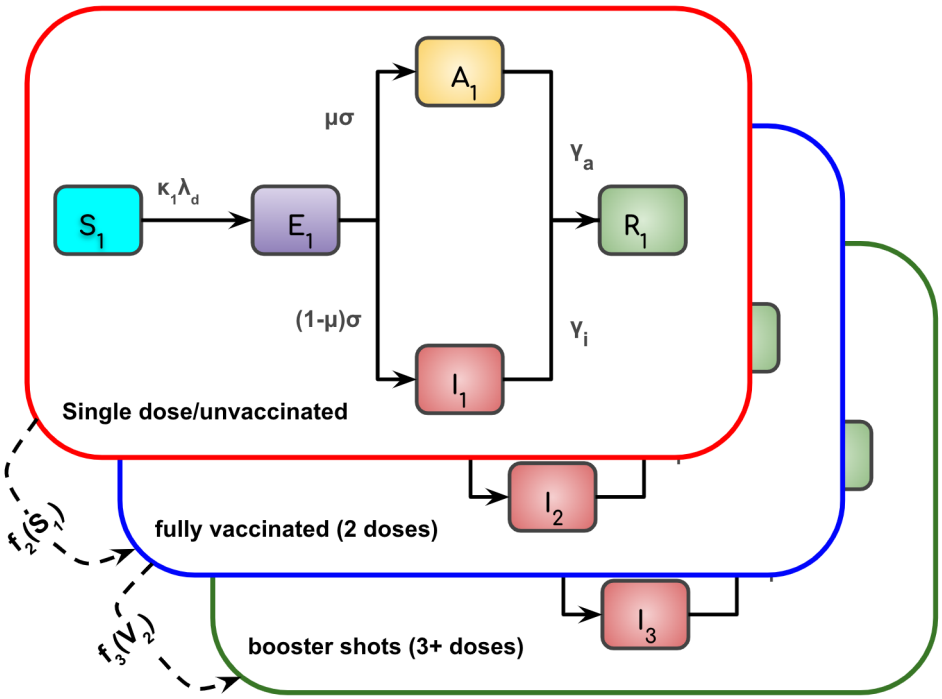

Fig 2. The SEAIR model with three vaccination cohorts. The vaccination cohorts are: unvaccinated/single-dose (cohort 1; red), fully vaccinated (cohort 2; blue), and booster-vaccinated (cohort 3; green). Each cohort contains susceptible, exposed, infectious (symptomatic and asymptomatic), and recovered compartments. Solid arrows show disease progression; dashed arrows show vaccination transitions $f_2(S_1)$ (cohort 1 to cohort 2) and $f_3(V_2)$ (cohort 2 to cohort 3).

given a contact relative to contact with a symptomatic individual. The combined

contributions from infectious individuals of all types and from all cohorts are defined by the force of infection, $\lambda_d(t)$, mathematically expressed as

$$\lambda_d(t) = \beta(t) \cdot \frac{\zeta A(t) + I(t)}{N} \tag{1}$$

where $\beta(t)$ is the estimated time-varying transmission rate defined by Eqn 2, $A(t) = A_1(t) + A_2(t) + A_3(t)$ is the total number of asymptomatic individuals across all cohorts, $I(t) = I_1(t) + I_2(t) + I_3(t)$ is the total number of symptomatic individuals across all cohorts. We do not include population demographics such as births and natural deaths due to the short period of the study. Also, we allow only individuals in the susceptible compartments to receive vaccination and transition to another vaccination cohort, because vaccination during infection is rare and unlikely to have any impact at the population level.

Descriptions of model parameters and their values are given in Table 1. Fitted parameters were specified with weakly informative priors (24; 25) centered on defined literature values and complete details are provided in Sec. S1.6 of S1 Text). As there was an active booster dose vaccination campaign during the study period, we modelled individuals moving between the susceptible compartments of the vaccination cohorts at rates based on PHAC vaccination data ((26); see Sec. S1.7 in S1 Text).

Table 1. Model parameters. Fixed parameters are estimated from published sources or data, and fitted parameters are estimated during model calibration. For details for $\beta(t)$ see 'Time-varying transmission rate'.

Symbol	**Definition**	**Value**	**Details**
		Fixed parameters	
N	Total population	510,550	(27)
μ	Proportion symptomatic	0.324	(28)
ζ	Relative infectiousness of asymptomatic cases	$\zeta = 0.75$; $(0 \leq \zeta \leq 1)$	(29)
κ_1	Susceptibility, unvaccinated	$\kappa_1 = 1.0$; $(0 \leq \kappa_1 \leq 1)$	(30)
		Fitted parameters	
σ	Rate from exposed to infectious	0.344 days^{-1}	Sec. S1.6 in S1 Text
γ_a	Recovery rate, asymptomatic	0.103 days^{-1}	Sec. S1.6 in S1 Text
γ_i	Recovery rate, symptomatic	0.144 days^{-1}	Sec. S1.6 in S1 Text
κ_2	Susceptibility, 2-dose vaccinated	$\kappa_2 = 0.90$; $(0 \leq \kappa_2 \leq 1)$	Sec. S1.6 in S1 Text
κ_3	Susceptibility, booster vaccinated	$\kappa_3 = 0.39$; $(0 \leq \kappa_3 \leq 1)$	Sec. S1.6 in S1 Text
		Time-varying parameters	
$v_2(t), v_3(t)$	Daily vaccination rates (2-dose & booster)	vaccination data	Sec. S1.7 in S1 Text
$\beta(t)$	Time-varying transmission rate	Eq. 2	see text

Time-varying transmission rate

To capture the changes in transmission over time, we modelled the time-varying transmission rate, $\beta(t)$, as a smooth exponential spline:

$$\beta(t) = \exp\left(b_0 + \sum_{i=1}^{N_B} b_i\, B_i(t)\right), \tag{2}$$

where t represents days since $t_s - 150$ as we begin fitting on t_s = December 15, 2021, and allow for a 150-day 'burn-in' period. The number of spline basis functions is N_B and the natural cubic spline basis functions are $B_i(t)$ with boundary knots at t_s and t_f, where t_f is May 22, 2022. The b_i parameters are spline coefficients that were estimated during the fitting. To regularize the spline and avoid extreme values, we generated the spline coefficients by sampling from the normal distribution with weakly informative priors (24; 25) centered on a biologically plausible value for the log-scale coefficients $\log(b_i)$, specified as

$$\log(b_i) \;\sim\; \begin{cases} \mathcal{N}\big(\log(\frac{1}{4}),\, 1\big), & \text{if } i = 0, \\ \mathcal{N}(0,\, 1), & \text{if } i = 1, \ldots, N_B. \end{cases}$$

Reproduction numbers for levels of the Alert Level System and K–12 school closures

To estimate the transmission rates across a period, $[t_a, t_b]$, corresponding to an alert level or school closure or opening, we considered all of the daily transmission rate estimates that occurred during this period. We computed the corresponding basic reproduction number as,

$$\mathcal{R}_0 = \bar{\beta}\big[t_a, t_b\big] \cdot \sum_{j=1}^{3} p_j \kappa_j \cdot \left(\frac{\mu}{\gamma_i} + \frac{(1-\mu)\zeta}{\gamma_a}\right)$$

where p_j is the proportion of the population in vaccination cohort j and

$$\bar{\beta}\big[t_a, t_b\big] = \frac{1}{t_b - t_a} \int_{t_a}^{t_b} \beta(t)\, dt,$$

is the mean transmission rate during the period of interest.

The vaccination campaign that was ongoing during our study period affected the reproduction number, so we calculated the reproduction number in a fully susceptible reference population to be able to compare the effect of NPIs without the confounding effect of ongoing vaccination. We reported 95% confidence intervals for all estimated quantities, including the transmission rate and the basic reproduction number, which were calculated using the Wald formula (estimate $\pm$ 1.96 $\times$ SE, with SE = SD/$\sqrt{n}$).

Model calibration

We calibrated the compartmental model to the weekly infection-induced seroprevalence estimates using December 15, 2021 as the start date (denoted t_s) and May 22, 2022 as the final date (denoted t_f). To simulate the epidemic dynamics, we solved the system of ordinary differential equations (ODEs, S1 Text in Sec. S1.5) using a fourth-order

Runge–Kutta (31) integration method with daily time steps from $t_s - 150$ to t_f. We allowed model simulations to begin 150 days before t_s to allow for a gradual buildup of infections such that the proportions of individuals in each compartment at the start of the fitting period t_s approaches their proportions at equilibrium. At 150 days before the start of the simulation $t_s - 150$, we initialized each vaccination cohort with one individual in each of the exposed, asymptomatic, symptomatic, and recovered states, and set the susceptible populations as $275,935$ (cohort 1) $234,601$ (cohort 2), and 1 (cohort 3). During the 150 day 'burn-in' period, vaccination occurred at rates given by the PHAC vaccination data, and on $t_s =$ December 15, 2021 this corresponds to vaccination in 82.5% (fully vaccinated, no booster doses) and 3.5% (fully vaccinated with booster doses) of the total NL population (510,543 people), which agrees with the PHAC vaccination data for this date.

We quantified the fit of observed weekly infection-induced seroprevalence estimates and model predictions as a Gaussian likelihood on the logit scale beginning from the start of the Omicron wave at $t_s =$ December 15, 2021. Specifically, we let X_j represent the observed seroprevalence proportion at time $t_j > t_s$. We obtain the model-predicted per capita number of recovered individuals as $R(t_j)/N$, where $R(t_j)$ is the cumulative number of recovered individuals across cohorts at time t_j and N is the population size. For each observation j, the likelihood contribution was defined as:

$$\text{logit}\big(X_j\big) \sim \mathcal{N}\left(\text{logit}\left(\frac{R(t_j)}{N}\right), \phi_X^2\right),$$

where ϕ_X is an unknown standard deviation parameter estimated from the seroprevalence data.

We fitted the model by maximizing the posterior distribution using the macpan2 (32) software package. macpan2 facilitates the estimation of compartmental models in R via Template Model Builder (TMB), a powerful tool for fitting complex latent-variable models. Confidence intervals for parameters, state trajectories, and fitted seroprevalence were computed via the delta method as implemented in macpan2.

Due to few community infections occurring initially during Omicron spread in NL, random events in small heterogeneous populations were impacting infection spread, and this could not be reproduced from our model. Therefore, we decided to only report results beginning on January 1, 2022 when infection had spread more substantially and these effects likely no longer persisted. For completeness, we show results beginning from the establishment of the Omicron variant on December 15, 2021, but results from before January 1, 2022 are shaded in grey and we de-emphasize the interpretation of results from this early period of infection spread.

Code to reproduce our results is available at `https://github.com/francisanokye/quantifying_omicron_burden_in_NL/tree/main`.

Results

The seroprevalence of SARS-CoV-2 increased from approximately 2% in early mid-December 2021 to slightly above 36% by late May 2022 (Fig 3). By 22, May 2022, a total of 193,263 infections were estimated from serosurveillance compared to the 41,508 that were reported. The first test eligibility period (T1) occurred during the early spread of the Omicron variant. The high underreporting estimate (4.1) for this period may reflect several factors, including the recent establishment of Omicron, a reporting anomaly that affected case counts, and limitations of our modelling approach when infection numbers are small. During the testing eligibility periods T2, T3, and T4, we estimated that the average underreporting ratio was 1.4, 2.5, and 2.9 unreported

infections per reported infection, respectively, and the underreporting ratios were relatively constant during this period (Fig 4B). During the testing eligibility period T5, the average underreporting ratio was 21.5 infections unreported for every 1 reported infection and the underreporting ratio increased from the beginning of the implementation of T5, reached a peak of more than 40 unreported infections per reported infection and then declined to just less than 30 unreported infections per reported infection at the end of the study period. The T5 period corresponds to when the eligibility for testing was restricted to high-risk symptomatic individuals or people who work with those at high-risk (Sec. S1.4 in S1 Text).

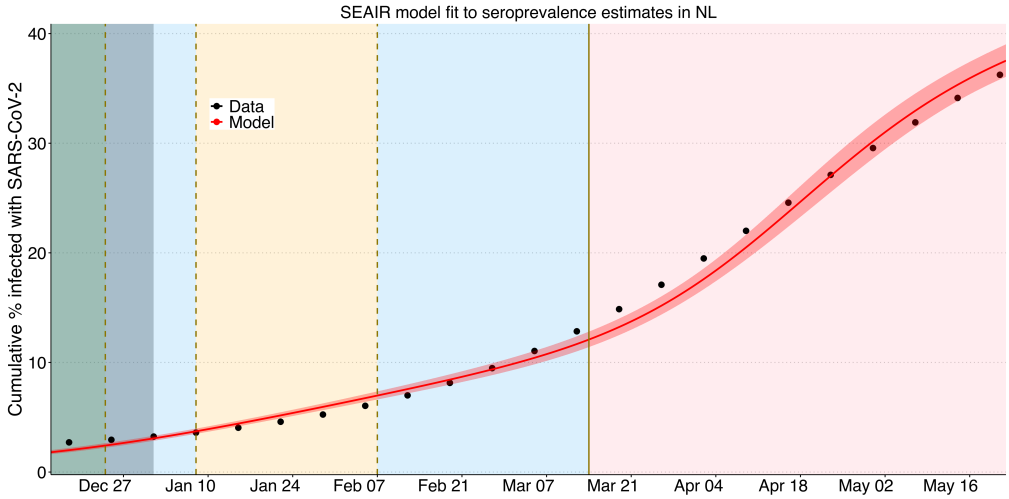

Fig 3. Model fit to infection-induced seroprevalence estimates from Dec 15, 2021 – May 22, 2022. Black dots are the reported seroprevalence estimates, and the red line with 95% confidence interval is the model-predicted percentage of the NL population that has recovered from infection. Shaded colours show different levels of NPIs under the ALS system (from least to most strict): No ALS (pink); ALS-2 (green), ALS-3 (blue); and ALS-4 (orange). The solid vertical line indicates the date on which the public health emergency declaration that instituted the ALS was repealed.

The estimated transmission rate $\beta(t)$ was lowest at 0.21 day^{-1} in the early stages of Omicron under ALS-3 when schools closed, but increased steadily from late January when schools opened, and peaked in early April after the repeal of the public health emergency declaration (No-ALS; Fig 5). The upward trend in transmission began despite ALS-4 being in place, coinciding with the reopening of K–12 schools and continuing through the shift to ALS-3 and into the No-ALS period. By early February, $\beta(t)$ increased from 0.27 day^{-1} (95% CI: 0.24–0.30 day^{-1}) to more than 0.35 day^{-1} (95% CI: 0.31–0.39 day^{-1}) by early March. The maximum transmission rate of 0.41 day^{-1} (95% CI: 0.36-0.47 day^{-1}) was observed in early April, after which the values declined but remained elevated between 0.29 and 0.33 day^{-1} through May. Overall, $\beta(t)$ ranged from a minimum of 0.21 day^{-1} to a maximum of 0.41 day^{-1}, such that the transmission rate nearly doubled during our study period.

Omicron transmission was found to be related to periods of school closures and the alert levels that were implemented. Periods when schools were closed consistently had lower levels of infection spread (mean $\mathcal{R}_0 = 1.44$, 95% CI: 1.41–1.47), compared to school-open periods (mean $\mathcal{R}_0 = 2.03$, 95% CI: 1.60–2.46; Fig 6A). When schools were open, $\mathcal{R}0$ varied across ALS phases, while when schools were closed, ALS-3 and ALS-4 produced nearly indistinguishable $\mathcal{R}_0$ transmission estimates. When ALS evaluation was performed independently of school operational status, the basic reproduction

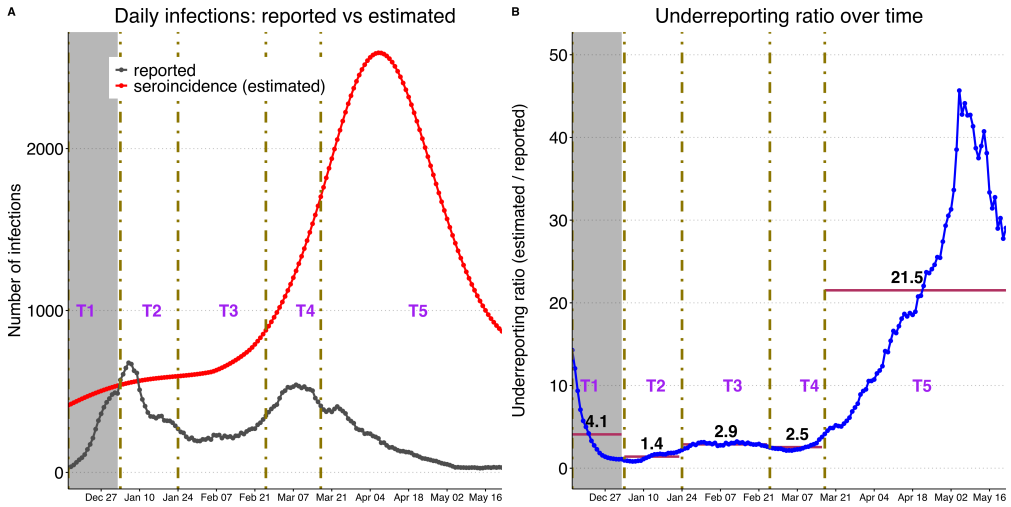

Fig 4. Daily reported cases, incidence inferred from serosurveillence, and the underreporting ratio during the Omicron wave in NL. (A) Model-predicted incidence as inferred from serosurveillance (red) and reported incidence (green) with changes in testing eligibility periods (T1–T5) shown as black dashed lines. (B) The daily underreporting ratio, calculated as daily estimated incidence divided by daily reported cases, with bars representing the mean ratio associated with each testing period. The grey shaded region is considered unrealiable due to a reporting anomaly.

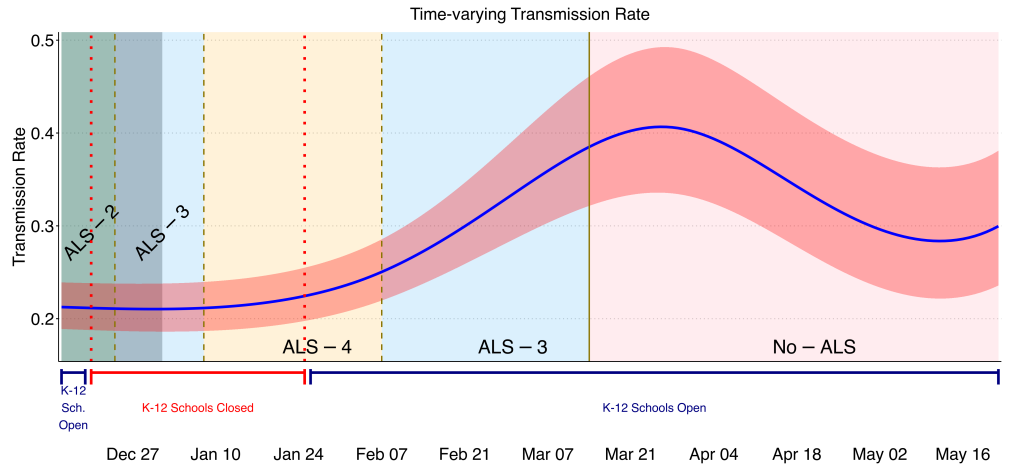

Fig 5. Estimated time-varying transmission rate for different NPIs. (A) Estimated daily transmission rate $\beta(t)$ (blue line) and its 95% confidence interval (shaded band). The vertical dashed lines indicate transition dates between levels of the ALS, and the solid vertical line marks the lifting of the public health emergency declaration. K–12 school status is shown below the horizontal axis indicating school closures (red) and openings (blue).

number, $\mathcal{R}_0$, differed across some of the different alert levels. The lowest basic reproduction number values were observed during ALS–4 (1.52, 95% CI: 1.35–1.69), higher values were observed during ALS–3 (2.12, 95% CI: 1.46–2.78), and the highest values were observed during the No–ALS phase (2.32, 95% CI: 1.69–2.95; Fig. 6B). These estimates indicate that the intensity of transmission increased progressively with the relaxation of the alert levels. We found more variability in transmission rates and $\mathcal{R}_0$ during ALS–3 and No–ALS, as these periods spanned longer durations.

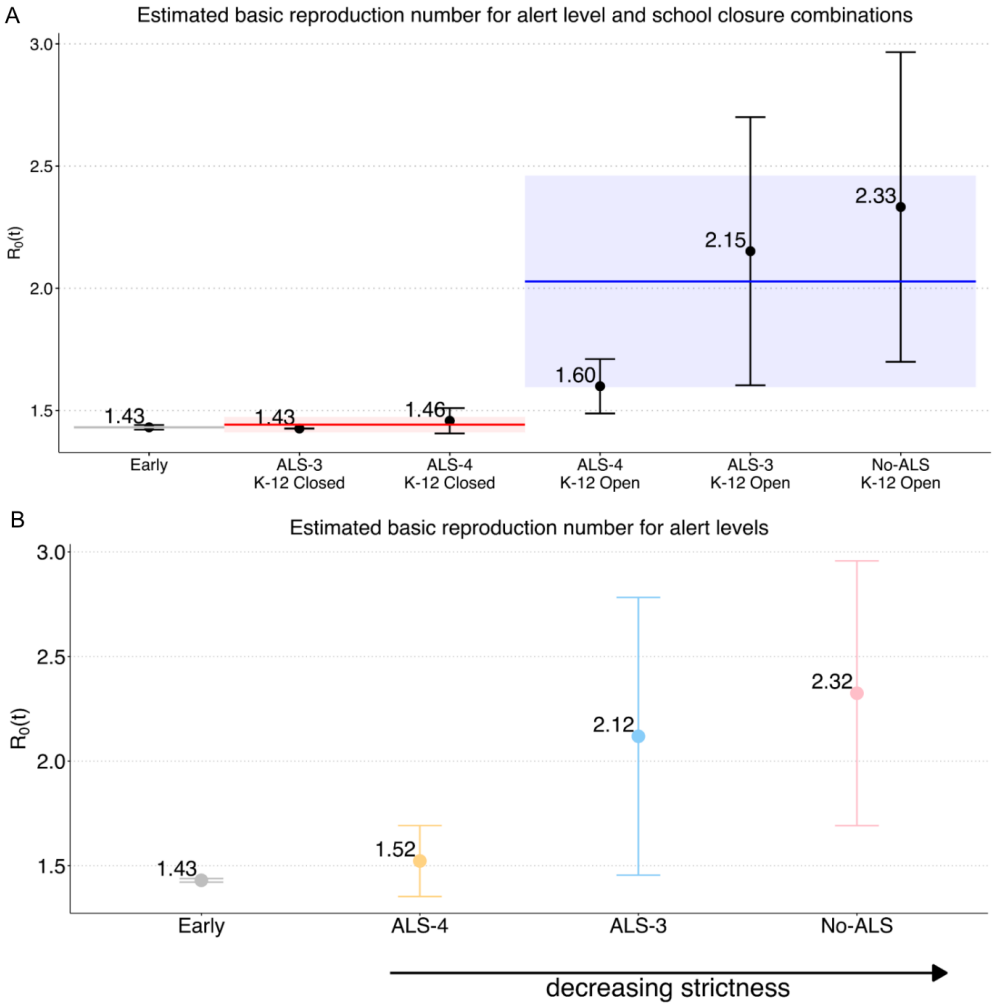

Fig 6. Estimated basic reproduction number $\mathcal{R}_0$ for different school closure and alert level combinations. Points indicate mean estimates, and vertical lines represent 95% confidence intervals.(A) Mean basic reproduction number $\mathcal{R}_0$ for alert level and K–12 school status combinations. Horizontal lines mark the overall mean $\mathcal{R}_0$ for each group: 1.44 [1.41–1.47] for school closures (red line) and 2.03 [1.60–2.46] for schools open (blue line). The basic reproduction number, $\mathcal{R}_0$, was consistently lower during K–12 closures and significantly higher after opening. (B) Overall $\mathcal{R}_0$ covering each alert level regardless of school operational status. The arrow indicates the direction of increasing restriction associated with each alert level.

Discussion

Consistent estimation of the number of infections is necessary to evaluate the impact of public health interventions during a pandemic. Our analysis considered serosurveillance data, as in Newfoundland and Labrador (NL), the highly transmissible Omicron variant overwhelmed PCR testing capacity, and testing eligibility changed several times during the study period. We found that the underreporting ratio was highest when testing eligibility was most restricted. During the period when testing eligibility was most restricted, the underreporting ratio increased substantially from fewer than 3 unreported infections per reported case to an average of more than 21 unreported infections per reported case (Fig. 4B). We also found that K–12 school closure and the strictest alert level (ALS-4) were associated with lower transmission. While NL had successfully controlled the original, alpha, and delta SARS-CoV-2 variants (7; 8), we found that none of the combinations of NPIs implemented during the spread of the Omicron variant resulted in estimates of $\mathcal{R}_0 < 1$ which would correspond to the ability to eliminate the Omicron variant in a wholly susceptible population.

The impact of NPIs implemented in Canada during the COVID-19 pandemic has been estimated by calibrating models to reported cases (33), but during the Omicron wave this was not possible because PCR testing capacity was exceeded in most jurisdictions (9) and the testing rate varied over time, such that the epidemiological curve based on reported cases did not reflect the actual epidemiological dynamics (34). While we estimate more than 40 underreported infections per reported infection (Fig. 4B) even higher underreporting ratios are estimated in British Columbia (Canada) over a corresponding time period (15).

For Ontario, an adjustment to reported cases that applied the testing rate of the most tested group to the entire Ontario population estimated 3.1 unreported cases for every reported case (between March 1, 2020 and September 4, 2022 (34)), and an adjustment based on model calibration to reported cases, hospitalizations, and deaths found 2.2 unreported cases per reported case (January 1–February 9, 2022 (9)). Bosco et al.'s estimate of 3.1 unreported infections per reported infection (34) is more consistent with our results, as their estimate of 3.1 applies to the entire period from March 2020 to September 2022, and these authors note that testing rates fell substantially from January 2022 onward, such that their underreporting ratio would exceed its average of 3.1 during our study period.

Furthermore, potentially explaining our high estimate of the underreporting ratio during T5 is that few Newfoundlanders and Labradorians had been infected with other SARS-CoV-2 variants, and so it is possible that there are a higher number of unreported infections than for Ontario, which had experienced more infections prior to the establishment of the Omicron variant. Across Canada, there was substantial variation in the dates when restrictive PCR eligibility criteria were implemented (Sec. S1.8 in S1 Text) after the establishment of the Omicron variant. NL's implementation on March 17, 2022 was the latest of all Canadian provinces with the exception of Prince Edward Island, which never limited PCR test eligibility to individuals in high-risk groups and that work with individuals in high-risk groups.

We found that in early January 2022, reported case counts briefly exceeded seroprevalence (Fig. 4A), but we note that this has been a characteristic of Canadian seroprevalence data, particularly during periods of, or for provinces with, low infection prevalence (see Sec. S1.9 in S1 Text). The alternative method of fitting the model to hospitalization and mortality data could not be applied in NL because hospitalizations and deaths were too few to use for model calibration.

After adjusting reported cases for under-testing, the first two pandemic waves in Ontario were equivalent in size, and three distinct pandemic waves occurred due to the emergence of the Omicron variant in 2022, when these characteristics of Ontario's

epidemiology during the COVID-19 pandemic were not present in the unadjusted reported case data (34). We found that the seroincidence curve for NL has just one peak in mid-April 2022, while reported cases peak in early January and again in early March, with a low occurring in mid-February. These highs and lows in reported cases correspond to periods when particular combinations of alert levels and school closures occurred in NL, such that fitting our model to reported cases would produce substantially different and erroneous conclusions regarding the relative efficacies of the different NPIs.

We found that K–12 school closures were associated with lower basic reproduction numbers (Fig. 6A) and that ALS-4 had the lowest basic reproduction number (Fig. 6B), which is reasonable as these lower reproduction numbers correspond to stricter NPIs. However, we also found that ALS-3 and No-ALS had similar reproduction numbers, even though No-ALS refers to the repeal of the Public Health Emergency declaration, when the ALS was no longer in place, and is less strict than ALS-3, which comprised an intermediate level of restrictions on gathering sizes and activities.

Shortly after the establishment of the Omicron variant in NL, we observed that the transmission rate was lower than at any other time, irrespective of the NPIs that were implemented (Fig. 5; left-most shaded grey). This may be reasonable, as NL had effectively controlled COVID-19 until the establishment of the Omicron variant, and the public may have exercised greater caution in response to the perceived unprecedented risk due to the establishment of the Omicron variant. Few Newfoundlanders and Labradorians had been infected with SARS-CoV-2 prior to the establishment of Omicron ($\sim$1.8% as of December 15, 2021; Table 1 and Fig. 3), and the high percentage of the NL population that was vaccinated suggests that most of the NL population followed public health directives to reduce the spread of SARS-CoV-2. Shortly after the establishment of the Omicron variant, in the Government of NL public briefings, it was stated that it was no longer possible to contact trace all SARS-CoV-2 infections (35) and that most people will contract the virus at some time (36). This combination of NL's low infection rate prior to Omicron, compliance with measures to limit the spread of the virus, and the high risk of Omicron variant infection may have resulted in voluntary actions that reduced the infection transmission rate, and this may explain why we estimate low transmission rates early in the outbreak.

Among the measures implemented, we observed that K–12 school closures were the most effective in reducing the Omicron variant transmission rate in NL, but these closures also occurred early in the outbreak, and this timing might explain our finding rather than the school closures themselves. Voluntary risk-reduction, uneven adherence to restrictions, and differences in contact patterns between age groups or settings likely influenced transmission, but could not be explicitly captured in our model. The limitation of our study in this aspect could have been mitigated if there were available data describing the NL population's behavioural response to the establishment of the Omicron variant, which might have occurred through surveys reporting age-structured contacts and attitudes or by measuring contacts and mobility.

Our SEAIR model considered many of the processes known to impact the spread of SARS-CoV-2, but a consistent barrier to our analysis was insufficient data. The reported case data alone are insufficient to disentangle the effects of individual NPIs during the Omicron wave, as these measures were implemented concurrently and are inherently correlated, making them difficult to capture within a simplified analysis framework. Hospitalizations and deaths were too few in NL for these data to be useful for calibration, making other data sources even more important. We calibrated our model to seroprevalence estimates, but these data were not available in real time to support decision-making. The vaccination data that we used has reporting gaps in the first weeks of our study, and data describing contacts, mobility, and behaviour were not

collected. During the public health emergency, resources were stretched, and this may explain the limited data, and yet improved data collection and sharing would enable analyses that could more definitely establish why the transmission rate was low after the initial establishment of the Omicron variant and inform public health strategies. Our analysis quantifies the impact of NPIs, which supports decisions (i.e., to enact or discontinue an ALS-4) and provides transparency that builds public trust and improves compliance with public health measures. Improving data collection and supporting modelling analysis of SARS-CoV-2 transmission would benefit future emergency responses.

S1 Text. Model equations, data and additional results. Provides full SEAIR model equations, parameter priors, and descriptions of seroprevalence, reported cases, vaccination uptake, and variant composition data. Includes supplementary figures (BA.1 dominance, reported cases vs. seroprevalence for all Canadian provinces, vaccination uptake) and tables (ALS measures, school closures, PCR testing eligibility, provincial PCR restrictions, and under-reporting ratios).

Acknowledgments

We thank the Newfoundland and Labrador Centre for Health Information (NLCHI, now part of NL Health Services – Digital Health) for providing access to the data (Health Research Ethics Board reference number 2021.013). We are also grateful to the COVID-19 Immunity Task Force (CITF) for serosurveillance, and to the public health officials and healthcare workers in Newfoundland and Labrador whose efforts in surveillance and reporting made this analysis possible.

References

1. World Health Organization. Tracking SARS-CoV-2 variants; 2023. `https://www.who.int/activities/tracking-SARS-CoV-2-variants`.

2. Viana R, Moyo S, Amoako DG, Tegally H, Scheepers C, Althaus CL, et al. Rapid epidemic expansion of the SARS-CoV-2 Omicron variant in southern Africa. Nature. 2022;603(7902):679–686.

3. Allan M, Lièvre M, Laurenson-Schafer H, De Barros S, Jinnai Y, Andrews S, et al. The World Health Organization COVID-19 surveillance database. International journal for equity in health. 2022;21(Suppl 3):167.

4. Shrestha LB, Foster C, Rawlinson W, Tedla N, Bull RA. Evolution of the SARS-CoV-2 omicron variants BA. 1 to BA. 5: implications for immune escape and transmission. Reviews in Medical Virology. 2022;32(5):e2381.

5. Wang H, Lan Y. The global dynamic transmissibility of COVID-19 and its influencing factors: an analysis of control measures from 176 countries. BMC Public Health. 2023;23(1):404.

6. Braeye T, Catteau L, Brondeel R, van Loenhout JA, Proesmans K, Cornelissen L, et al. Vaccine effectiveness against transmission of alpha, delta and omicron SARS-COV-2-infection, Belgian contact tracing, 2021–2022. Vaccine. 2023;41(20):3292–3300.

7. Hurford A, Martignoni MM, Loredo-Osti JC, Anokye F, Arino J, Husain BS, et al. Pandemic modelling for regions implementing an elimination strategy. Journal of Theoretical Biology. 2023;561:111378.

8. Doig R, Hurford A, Spurrell S, Morrissey A, Wang L, Colijn C. Changing contact patterns in Newfoundland and Labrador, Canada in repsonse to public health measures during the COVID-19 pandemic. MedRxiv. 2025;.

9. Yuan P, Aruffo E, Tan Y, Yang L, Ogden NH, Fazil A, et al. Projections of the transmission of the Omicron variant for Toronto, Ontario, and Canada using surveillance data following recent changes in testing policies. Infectious Disease Modelling. 2022;7(2):83–93.

10. Martignoni MM, Mohammadi Z, Loredo-Osti JC, Hurford A. Extensive SARS-CoV-2 testing reveals BA. 1/BA. 2 asymptomatic rates and underreporting in school children. Canada Communicable Disease Report. 2023;49(4):155.

11. Corman VM, Landt O, Kaiser M, Molenkamp R, Meijer A, Chu DK, et al. Detection of 2019 novel coronavirus (2019-nCoV) by real-time RT-PCR. Eurosurveillance. 2020;25(3):2000045.

12. Shioda K, Lau MS, Kraay AN, Nelson KN, Siegler AJ, Sullivan PS, et al. Estimating the cumulative incidence of SARS-CoV-2 infection and the infection fatality ratio in light of waning antibodies. Epidemiology. 2021;32(4):518–524.

13. Murphy TJ, Swail H, Jain J, Anderson M, Awadalla P, Behl L, et al. The evolution of SARS-CoV-2 seroprevalence in Canada: a time-series study, 2020–2023. Cmaj. 2023;195(31):E1030–E1037.

14. Havers FP, Reed C, Lim T, Montgomery JM, Klena JD, Hall AJ, et al. Seroprevalence of antibodies to SARS-CoV-2 in 10 sites in the United States, March 23-May 12, 2020. JAMA Internal Medicine. 2020;180(12):1576–1586.

15. Skowronski DM, Kaweski SE, Irvine MA, Kim S, Chuang ES, Sabaiduc S, et al. Serial cross-sectional estimation of vaccine-and infection-induced SARS-CoV-2 seroprevalence in British Columbia, Canada. CMAJ. 2022;194(47):E1599–E1609.

16. He X, Chen H, Zhu X, Gao W. Non-pharmaceutical interventions in containing COVID-19 pandemic after the roll-out of coronavirus vaccines: a systematic review. BMC Public Health. 2024;24(1):1524.

17. COVID-19 Immunity Task Force. Mandate & Strategy; 2024. `https://www.covid19immunitytaskforce.ca/mandate-strategy/`.

18. Public Health Agency of Canada. COVID-19 epidemiology update – Canada (archived 2022-10-07); 2022. `https://health-infobase.canada.ca/covid-19/archive/2022-10-07/`.

19. Government of Newfoundland and Labrador. NL COVID-19 Alert Level System: Implications for Municipalities; 2020. `https://www.gov.nl.ca/ecc/files/NL-COVID-Table-for-MNL-Final-March-2021.pdf`.

20. Government of Newfoundland and Labrador. NL Public Health Orders; 2020. `https://www.gov.nl.ca/covid-19/updates-resources/previous-public-health-orders/`.

21. Tuite AR, Fisman DN, Greer AL. Mathematical modelling of COVID-19 transmission and mitigation strategies in the population of Ontario, Canada. Cmaj. 2020;192(19):E497–E505.

22. Xue L, Jing S, Wang H. Evaluating the impacts of non-pharmaceutical interventions on the transmission dynamics of COVID-19 in Canada based on mobile network. PLoS One. 2021;16(12):e0261424.

23. Vilches TN, Abdollahi E, Cipriano LE, Haworth-Brockman M, Keynan Y, Sheffield H, et al. Impact of non-pharmaceutical interventions and vaccination on COVID-19 outbreaks in Nunavut, Canada: a Canadian Immunization Research Network (CIRN) study. BMC Public Health. 2022;22(1):1042.

24. Gelman A. Prior distributions for variance parameters in hierarchical models (comment on article by Browne and Draper). 2006;.

25. Lemoine NP. Moving beyond noninformative priors: why and how to choose weakly informative priors in Bayesian analyses. Oikos. 2019;128(7):912–928.

26. Public Health Agency of Canada. Canadian COVID-19 vaccination coverage report; 2024. `https://health-infobase.canada.ca/covid-19/vaccination-coverage/`.

27. Statistics Canada. Census Profile. 2021 Census of Population; 2022. `https://www12.statcan.gc.ca/census-recensement/2021/dp-pd/prof/index.cfm?Lang=E`.

28. Shang W, Kang L, Cao G, Wang Y, Gao P, Liu J, et al. Percentage of asymptomatic infections among SARS-CoV-2 omicron variant-positive individuals: a systematic review and meta-analysis. Vaccines. 2022;10(7):1049.

29. Johansson MA, Quandelacy TM, Kada S, Prasad PV, Steele M, Brooks JT, et al. SARS-CoV-2 transmission from people without COVID-19 symptoms. JAMA network open. 2021;4(1):e2035057–e2035057.

30. Andrews N, Stowe J, Kirsebom F, Toffa S, Rickeard T, Gallagher E, et al. Covid-19 vaccine effectiveness against the Omicron (B. 1.1. 529) variant. New England Journal of Medicine. 2022;386(16):1532–1546.

31. Butcher J. Runge–Kutta methods for ordinary differential equations. Numerical Analysis and Optimization: NAO-III, Muscat, Oman, January 2014. 2015; p. 37–58.

32. Steve Walker, Weiguang Guan, Jen Freeman, Ben Bolker, Darren Flynn-Primrose. macpan2: Fast and Flexible Compartmental Modelling; 2025. Available from: `https://canmod.github.io/macpan2/`.

33. Ogden NH, Turgeon P, Fazil A, Clark J, Gabriele-Rivet V, Tam T, et al. Counterfactuals of effects of vaccination and public health measures on COVID-19 cases in Canada: What could have happened? Canada Communicable Disease Report. 2022;48(7-8):292.

34. Bosco S, Peng A, Tuite AR, Simmons A, Fisman DN. Impact of adjustment for differential testing by age and sex on apparent epidemiology of SARS-CoV-2 infection in Ontario, Canada. BMC infectious diseases. 2025;25(1):589.

35. Government of Newfoundland and Labrador. Report to the House of Assembly on the COVID-19 Public Health Emergency; 2022. `https://www.assembly.nl.ca`.

36. CBC News. As N.L. warns of COVID-19's inevitability, immunocompromised people fear they've been forgotten; 2022. https://www.cbc.ca/lite/story/1.6307769.